Monodisperse ZnFe2O4 nanospheres synthesized by a nonaqueous route for a highly slective low-ppm-level toluene gas sensor

Dong, Chengjun; Liu, Xu; Xiao, Xuechun; Du, Shangfeng; Wang, Yude

DOI:
10.1016/j.snb.2016.09.122

Document Version
Peer reviewed version

Citation for published version (Harvard):
Dong, C, Liu, X, Xiao, X, Du, S & Wang, Y 2017, 'Monodisperse ZnFe2O4 nanospheres synthesized by a nonaqueous route for a highly slective low-ppm-level toluene gas sensor', Sensors and Actuators B: Chemical, vol. 239, pp. 1231-1236. https://doi.org/10.1016/j.snb.2016.09.122

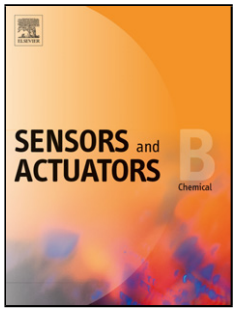

Title: Monodisperse $ZnFe_2O_4$ nanospheres synthesized by a nonaqueous route for a highly slective low-ppm-level toluene gas sensor

Author: Chengjun Dong Xu Liu Xuechun Xiao Shangfeng Du Yude Wang

PII: S0925-4005(16)31547-7
DOI: http://dx.doi.org/doi:10.1016/j.snb.2016.09.122
Reference: SNB 20988

To appear in: *Sensors and Actuators B*

Received date: 10-6-2016
Revised date: 14-9-2016
Accepted date: 21-9-2016

Please cite this article as: Chengjun Dong, Xu Liu, Xuechun Xiao, Shangfeng Du, Yude Wang, Monodisperse ZnFe2O4 nanospheres synthesized by a nonaqueous route for a highly slective low-ppm-level toluene gas sensor, Sensors and Actuators B: Chemical http://dx.doi.org/10.1016/j.snb.2016.09.122

Monodisperse $ZnFe_2O_4$ nanospheres synthesized by a nonaqueous route for a highly slective low-ppm-level toluene gas sensor

Chengjun Dong,[a] Xu Liu,[a] Xuechun Xiao,[a] Shangfeng Du,[b] Yude Wang [c,*]

a School of Materials Science and Engineering, Yunnan University, 650091 Kunming, People's Republic of China.

b School of Chemical Engineering, University of Birmingham, Edgbaston, Birmingham B15 2TT, UK.

c Department of Physics, Yunnan University, 650091 Kunming, People's Republic of China.

[*] To whom correspondence should be addressed. Tel:+86-871-65035570; Fax: +86-871-65035376. E-mail: ydwang@ynu.edu.cn (Y. D. Wang)

Graphical abstact

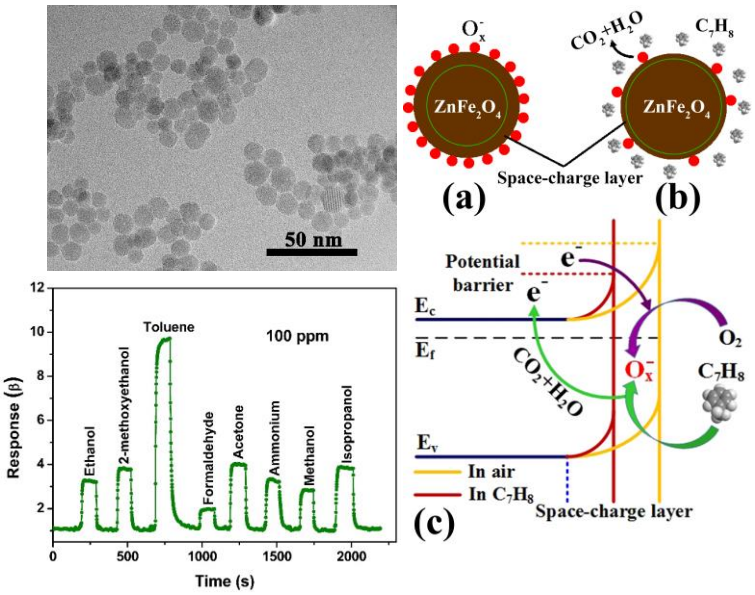

Highlights

- Monodisperse $ZnFe_2O_4$ nanospheres were synthesized via a nonaqueous route.
- $ZnFe_2O_4$ nanospheres have diameters of 7-16 nm and a large surface area of 87.40 m^2/g.
- $ZnFe_2O_4$ nanospheres show a high pontential for detecting low-ppm-level toluene.
- $ZnFe_2O_4$ nanospheres exhibit good linearity with a high response and excellent selectivity.

Abstract

Monodisperse $ZnFe_2O_4$ nanospheres were succesuffully synthesized via a nonaqueous route in benzyl alcohol at low temperaure of 200 °C. It was found that the $ZnFe_2O_4$ is 7-16 nm in diameter with a large surface area of 87.40 m^2/g. The gas sensor based on $ZnFe_2O_4$ nanospheres shows a high pontential for detecting low-ppm-level toluene, exhibiting a good linearity ranging from 1-100 ppm with a high response (100 ppm: 9.98) and excellent selectivity.

Keywords: $ZnFe_2O_4$ nanospheres; Nonaqueous synthesis; Gas response; Toluene; Low-ppm-level; Selectivity

1. Introduction

Toluene (C_7H_8) is widely used in chemical industry and found to be neurotoxi, which is harmful to human beings even at a very low concentration [1]. An effective detection of toluene gas is of great benefit to both the environment and our own humanity. Many sensing materials such as SnO_2 [2], ZnO [3], WO_3 [4], α-Fe_2O_3 [5], In_2O_3 [6], Co_3O_4 [7], CuO [8], etc., and their hybrids [9,10] have been prepared for toluene detection. However, a highly selective detection of low-ppm-level toluene still remains a great challenge. As a multifunctional n-type semiconductor, $ZnFe_2O_4$ has attracted much attention in the fields of gas sensors, catalysts, magnets, Li-ion batteries and solar cells [11-18]. In particular, the excellent gas-sensing properties of various $ZnFe_2O_4$ materials have been extensively explored in recent years. For instance, the earlier works have been demonstrated, such as $ZnFe_2O_4$ particles to H_2S [14], ultrafine powder to Cl_2 [15], $ZnFe_2O_4$/ZnO to n-butanol [16], porous $ZnFe_2O_4$ nanoshpheres to acetone [17], and so on. However, the sensing performances of $ZnFe_2O_4$ towards toluene is yet reported but highly fascinating.

$ZnFe_2O_4$ nanostructures have been prepared through various apporachs and investigated for diverse purposes. In which, nonaqueous approaches in organic solvents under exclusion of water have been reported to offer many advantages in controlling synthesis. The organic component in the reaction mixture not only acts as the oxygen supplying agent but also strongly influences products in terms of their particle size, shape, surface and assembly properties [19-21]. Many metal oxide nanoparticles, hybrid nanomaterials, aerogel and thin films with different shapes and sizes have been prepared based on the nonaqueous approach [19-25]. A solvent of benzyl alcohol has typically been used, the group of Niederberger in

particular, to prepare nanocrystals of different metal oxides [19,23,24]. The benzyl alcohol prevents the use of any surfactants and itself may play a multiple role as reaction medium, oxygen supplying and/or capping agent [19].

In this commnication, we report the synthesis of monodisperse $ZnFe_2O_4$ nanospheres by a nonaqueous route and its application for toluene detection. The synhesis was performed at 200 ℃ for 24 h using nonaqueous zinc acetate and Iron (Ⅲ) acetylacetonate as precursors and benzyl alchol as oxygen supplying agent. The obtained $ZnFe_2O_4$ nanopheres was characterized via X-ray diffraction, transmission electron microscopy (TEM), and X-ray photoelectron spectroscopy (XPS). The high sensitivity and excellent selectivity of the $ZnFe_2O_4$ nanospheres towards toluene detection was evaluated at the operating temperatrue of 300 ℃.

2. Experimental section

2.1 Materials synthesis

All of the analytical grade reagents in this work were purchased from Aladdin and were used directly without any further purification. A typical preparation procedure was as follows: 1 mmol nonaqueous Zinc acetate and 2 mmol Iron (III) acetylacetonate were dissolved in 30 ml benzyl alcohol under stirring for 30 min. Subsequently, the resulting solution was transferred into 50 ml Teflon-lined stainless-steel autoclave. The crystallization was carried out at 200 ℃ for 24 h. When the autoclave was cooled naturally down to room temperature, the products were washed thoroughly with acetone, ethanol, and deionized water for several times. The final $ZnFe_2O_4$ powder was collected after dried at 60 ℃.

2.2 *Materials characterization*

The crystal structure and phase identification of the as-synthesized $ZnFe_2O_4$ were estimated by X-ray diffraction (XRD, Rigaku TTRIII) using Cu K_α 1 radiation (with an incident X-ray wavelength of 1.54056 Å). The energy-dispersive X-ray spectroscopy (EDX) was carried out by a FEI QUANTA 200 equipped with an EDX attachment. Transmission electron microscopy (TEM) and high-resolution transmission electron microscopy (HRTEM) measurements were performed on a JEM-2100 (JEOL, Japan) at an operating acceleration voltage of 200 kV. X-ray photoelectron spectroscopy (XPS) analysis was conducted using ESCALAB system with Al K_α X-ray radiation under a working voltage of 15 kV. The specific surface area of the as-prepared material was tested using Nitrogen adsorption isotherm method at 77.3 K with a Micromeritics ASAP 2010 automated sorption analyzer. Before the measurement, the sample was degassed under vacuum at 300 °C for 3 h.

2.3 Gas sensor preparation and measurement

The as-synthesized $ZnFe_2O_4$ nanospheres were used to fabricate gas sensors as following. A certain amount of products were firstly grinded with an appropriate amount of deionized water to form a paste. Then, the paste was carefully painted onto the outside surface of an alumina tube (4 mm in length, 1.2 mm in outside diameter, and 0.8 mm in internal diameter) with a pair of Au electrodes at each end connected by platinum wires. The thickness of sensing materials was about 0.6-0.8 mm.

After being calcined in air at 400 ^oC for 1 h, a Ni-Cr heating wire was put through the tube and all wires were carefully connected to a Bakelite base to perform electrical measurements using a WS-30 A system. More details were described in the Supplementary Material. For a typical n-type gas sensor, the response (β) was defined as the ratio (R_a/R_g) of

the sensor resistance in dry air (R_a) to that of analytic gas (R_g). The response and recovery times are defined as the time required to reach 90% of the initial equilibrium value.

3. Results and discussion

XRD pattern of the as-synthesized $ZnFe_2O_4$ sample is shown in Fig. 1. All peaks are well indexed to a cubic $ZnFe_2O_4$ structure (JPCDS Card No. 74-2397) with space group $Fd\bar{3}m$, indicating no secondary phase formed in the synthesis process. The Rietveld refinement of XRD pattern was conducted using the commonly accepted Maud program developed by Luca Lutterotti [26]. The calculated XRD profile fits well with the experimental data cross the whole tested angles from 10-80°. The structural parameters obtained from the Rietveld refinement are listed in Table S1 in the Supplementary Material. The lattice constant is refined to be 8.4374 Å, which is in close agreement with the standard JCPDS value of 8.4432 Å (JPCDS Card No. 74-2397). Furthermore, the average crystallite size was estimated as 14.5 nm as shown by the broadening XRD peaks. In addition, the EDX results confirm that it is mainly composed Zn, Fe, and O (Fig. S2) with ratio of about 1:2:4, matching the chemical formula of $ZnFe_2O_4$.

TEM and HRTEM images are displayed in Fig. 2 to show the fine microstructure of $ZnFe_2O_4$ product. As expected, the TEM images (Fig. 2 (a) and (b)) show that the $ZnFe_2O_4$ appears spherical-like morphology with either isolated or as bundles. The diameter of the nanospheres is approximately 7 to 16 nm. HRTEM image of an individual nanosphere (Fig. 2(c)) exhibits sets of lattice fringes with an interplanar distance of 0.478 nm, which is in line with that of (111) facet of $ZnFe_2O_4$. From the selected-area electron diffraction (SAED) pattern shown in Fig. 2 (d), diffraction rings are identified as the reflections (111), (220),

(311), (222), (511), and (440) of cubic $ZnFe_2O_4$. These findings give additional evidence that the obtained $ZnFe_2O_4$ nanospheres are highly crystallized, further supporting the above XRD results.

The specific surface area of the $ZnFe_2O_4$ nanospheres is examined by the nitrogen adsorption-desorption isotherms measurement and a value of 87.40 m^2/g was achieved. This large accessible surface area can provide much more active sites for the gas molecules' reaction and hence excellent gas-sensing performances are expected.

The surface chemical states of $ZnFe_2O_4$ nanospheres were analyzed by XPS (Fig. S5), and core levels of Zn 2p, Fe 2p and O 1s could be identified. Two peaks of Zn $2p_{3/2}$ and Zn $2p_{1/2}$ located at 1022.05 eV and 1045.10 eV with a better symmetry, implying the formation of Zn^{2+} [27]. The XPS of the Fe 2p region is fitted into four contributions. The first two peaks with the binding energy (BE) values of about 712.30 and 719.54 eV are assigned to Fe $2p_{3/2}$ and its shakeup satellite, while the higher BE peaks around 726.02 eV and 734.03 eV correspond to Fe $2p_{1/2}$ and its shakeup satellite, respectively, indicating the presence of the Fe^{3+} cations [28]. In particular, the state of O 1s is well evolved into two distinguishable peaks with BE values of about 530.69 eV (lattice oxygen: $O_{lattice}$) and 532.30 eV (adsorbed oxygen: O_{ads}), respectively. The adsorbed oxygen is widely considered to play a critical role for gas detection.

To understand the gas-sensing properties towards toluene, sensors were constructed from the as-prepared $ZnFe_2O_4$ nanospheres. As shown in Fig. S3 and Table S2, we made comparison between response, response time and recovery time to 100 ppm toluene at typical temperature. At low temperature such as 260 °C, the response is 79.12, but the gas

sensor takes much longer time to response (>156 s) and recovery (383 s). At higher temperature of 340 ℃, although the fast response (6 s) and recovery (8 s) can be obtained, the response reduces to be 3.8. Therefore, taking the gas-sensing properties such as response, response and recovery time, etc., into the overall consideration, an operating temperature of 300 ℃ was chosen. Fig. 3 (a) shows the actual resistance of the $ZnFe_2O_4$ sensor exposed to various concentrations of toluene gas ranging from 1-100 ppm. As can be seen, the sensors demonstrated a reduced resistance upon exposure to toluene, typically observing in n-type semiconductor gas sensors. It can be seen that even a very low concentration of toluene, i.e. 1 ppm, can be effectively detected. The corresponding responses are 1.41, 1.83, 2.20, 3.85, 5.15, 6.75, and 9.98 to 1, 5, 10, 30, 50, 70, and 100 ppm toluene, respectively, as plotted in Fig. 3(b). The relationship between the response and toluene concentration (1-100 ppm) shows a very good linearity, that is $\beta=0.08C+1.29$ (here β is the response and C is the toluene concentration) with a relative correlative coefficient R^2=0.991 by lineal fitting of the experimental data. The response time and recovery time of the sensor are calculated to be 18.14 and 29.20 s towards 100 ppm toluene, as shown in Fig. 3(c). In addition, the reproducibility of $ZnFe_2O_4$ sensor was also studied with 100 ppm toluene gas. In Fig. 3(d), the reproducibility test demonstrates that the sensor nearly maintains its initial value of response without a big fluctuation upon five successive sensing tests. Besides, a long-term stability of the $ZnFe_2O_4$ based sensor has been tested. As shown in Fig. S 4, the sensor exhibits a good stability towards 50 ppm and100 ppm toluene in 20 days. The mean response are calculated to be 5.23 and 9.99 with changes of ±17% and ±11 % for 50 ppm and 100 ppm toluene, respectively. These findings verify our sensor could possess excellent stability

in long term. Previous reports in open literatures about various sensing materials based toluene sensors with distinct morphologies are compared in Table S3. Obviously, the $ZnFe_2O_4$ nanospheres based sensor in our work possesses a comparable sensing-performance towards toluene.

The selectivity of sensors is also considered as one of the important parameters in their practical applications in guaranteeing exact recognition of a specific target molecule among various gases. Therefore, the response of the $ZnFe_2O_4$ based sensor to different gases, including ethanol, 2-methoxyethanol, toluene, formaldehyde, acetone, ammonium, methanol and isopropanol, was tested towards a fixed concentration of 100 ppm at the same operating temperature, as comparably summarized in Fig. 4. Apparently, the $ZnFe_2O_4$ based sensor exhibits a much higher sensitivity to toluene rather than to other tested gases. Several factors might be attributed to the good selectivity with respect to both toluene molecules and $ZnFe_2O_4$. Firstly, it is probable that the methyl group ($-CH_3$) played an important role in enhancing the sensing behavior because of its adsorbing ability [29]. Secondly, lower enthalpy change of the dehydrogenation for toluene possibly results in higher response [30]. Moreover, the small energy difference in terms of lowest unoccupied molecule orbit (LUMO) energy and highest occupied molecule orbit (HUMO) energy between toluene and $ZnFe_2O_4$ could favor the interaction to take place, which is contributed to the good selectivity of toluene [31].

The gas-sensing mechanism of $ZnFe_2O_4$ nanospheres can be detailed by following the classical electron depletion theory [32,33] and visibly displayed in Fig. 5. In air, oxygen molecules adsorb on the surface of the sensing materials, and thus capture electrons from the

conduction band of $ZnFe_2O_4$ to create oxygen species O_{ads} (such as O^-, O^{2-}, and O_-), as shown in XPS analysis (Fig. S5). As a result, the charge concentrations decrease, leading to a widening thickness of the charge accumulation layer (the increase of R_a) (Fig. 5 (a)). After exposing to reducing gas like toluene, toluene molecules react with the adsorbed oxygen species, which is $C_7H_8 + O_{ads} \rightarrow CO_2 + H_2O$, releasing the trapped electrons back into $ZnFe_2O_4$. Thus the charge concentrations will increase and the thickness of the charge accumulation layer decrease accordingly (the decrease of R_g) (Fig. 5 (b)). Accompanying with the variation of electrons, a contrastive change of the potential barrier as well as space-charge layer are compared in Fig. 5 (c), which is the essence of a semiconductor gas sensor. In brief, the change of resistance is definitely dependent on the sensing material, the chemisorbed oxygen and the tested gas. In our case, the relatively strong interaction between the toluene molecules and the surface oxygen species of $ZnFe_2O_4$ is the plausible reason for the excellent sensing performance.

Taken together, these results indicate that the $ZnFe_2O_4$ nanospheres are a promising gas sensing material in detecting low concentration toluene gas in the environment. The good sensing performance is attributed to its native nature, and in particular the high surface area which enables a large exposure of surface atoms to provide more active sites for the absorption of gas molecules and hence facilitate the surface reactions. Very recently, the detection of ppb-level toluene was realized with Pt-functionalized SnO_2-ZnO core-shell nanowires [9]. Hence, more works are highly desired to further improve the performance of $ZnFe_2O_4$ nanospheres based sensor by coupling with other sensing materials, doping with approated elements, or functionalizing with noble nanoparticles.

4. Conclusions

In summary, $ZnFe_2O_4$ nanospheres with 7-16 nm in diameter was prepared by a one-pot solverthermal route using benzyl alcohol as solvent. The native nature and in particular the large specific surface area, 87.40 m^2/g, were favorable for the gas sensing performance. Gas-sensing measurements indicated that the $ZnFe_2O_4$ nanospheres based sensor exhibits a high response and excellent selectivity to the detection of low-ppm-level toluene gas, with a response of 1.41 and 9.98 at 1 and 100 ppm, respectively. A good linearity was achieved within the range of 1-100 ppm. The excellent detection performance, in addition with the simple preparation approach, makes the as-synthesized $ZnFe_2O_4$ nanospheres a promising material for toluene gas detection at a low concentration.

Acknowledgements

This work was supported by the National Natural Science Foundation of China (No. 51262029) and the Project of the Department of Education of Yunnan Province (2015Y008).

Appendix A. Supplementary data

Supplementary data associated with this article can be found, in the online version, at doi:.

References

[1] World Health Organization, Air quality guidelines for Europe, 2000.

[2] J. R. Huang, X. J. Xu, C. P. Gu, W. Z. Wang, B. Y. Geng, Y. F. Sun, J. H. Liu, Effective VOCs gas sensor based on porous SnO_2 microcubes prepared via spontaneous phase segregation, *Sensors and Actuators B* 173 (2012) 599–606.

[3] L. W. Wang, S. R. Wang, M. J. Xu, X. J. Hu, H. X. Zhang, Y. S. Wang, W. P. Huang, A Au-functionalized ZnO nanowire gas sensor for detection of benzene and toluene, *Physical Chemistry Chemical Physics* 15 (2013) 17179–17186.

[4] Z. H. Li, J. C. Li, L. L. Song, H. Q. Gong, Q. Niu, Ionic liquid-assisted synthesis of WO 3 particles with enhanced gas sensing properties, *Journal of Materials Chemistry A* 1 (2013) 15377–15382.

[5] S. R. Wang, Y. S. Wang, H. X. Zhang, X. L. Gao, J. D. Yang, Y. Wang, Fabrication of porous α-Fe_2O_3 nanoshuttles and their application for toluene sensors, *RSC Adv*ances 4 (2014) 30840–30849.

[6] Z. H. Li, Y. L, Y. X. Luan, J. C. Li, A. X. Song, In $(OH)_3$ particles from an ionic liquid precursor and their conversion to porous In_2O_3 particles for enhanced gas sensing properties, *CrystEngComm* 15 (2013) 1706–1714.

[7] C. H. Zhao, B. Y. Huang, J. Y. Zhou, E. Q. Xie, Synthesis of porous Co_3O_4 nanonetworks to detect toluene at low concentration, *Physical Chemistry Chemical Physics* 16 (2014) 19327–19332.

[8] C. Yang, F. Xiao, J. D. Wang, X. T. Su, A highly sensitive colorimetric sensor for

adrenaline detection based on organic molecules-functionalized gold nanoparticles, *Sensors and Actuators B* 207 (2015) 277–285.

[9] J. H. Kim, S. S. Kim, Realization of ppb-scale toluene-sensing abilities with Pt-functionalized SnO_2-ZnO core-shell nanowires, *ACS Appl. Mater. Interfaces*, 7 (2015) 17199–17208.

[10] H. Shan, C. B. Liu, L. Liu, J. B. Zhang, H. Y. Li, Z. Liu, X. B. Zhang, X. Q. Chi, Excellent toluene sensing properties of SnO_2-Fe_2O_3 interconnected nanotubes, *ACS Appl. Mater. Interfaces*, 5 (2013) 6376–6380.

[11] L. Lin, Q. M. Pan, $ZnFe_2O_4$@ C/graphene nanocomposites as excellent anode materials for lithium batteries, *Journal of Materials Chemistry A* 3 (2015) 1724–1729.

[12] J. A. Gomes, G. M. Azevedo, J. Depeyrot, J. Mastnik-Filh, F. L. O. Paula, F. A. Torunhl, R. Perzynski, Structural, chemical, and magnetic investigations of core–shell zinc ferrite nanoparticles, *Journal of Physical Chemistry C* 116 (2012) 24281–24291.

[13] R. Dom, R. Subasri, N. Y. Hebalkar, A. S. Chary, P. H. Borse, Synthesis of a hydrogen producing nanocrystalline $ZnFe_2O_4$ visible light photocatalyst using a rapid microwave irradiation method, *RSC Advances* 2 (2012) 12782–12791.

[14] C. V. Gopal Reddy, S. V. Manorama, V. J. Rao, Preparation and characterization of ferrites as gas sensor materials, *Journal of Materials Science Letters* 19 (2000) 775–778.

[15] X. S. Niu, W. P. Du, W. M. Du, Preparation and gas sensing properties of ZnM_2O_4 (M= Fe, Co, Cr), *Sensors and Actuators B* 99 (2004) 405–409.

[16] S. R. Wang, J. X. Zhang, J. D. Yang, X. L. Gao, H. X. Zhang, Y. S. Wang, Z. Y. Zhu,

Spinel $ZnFe_2O_4$ nanoparticle-decorated rod-like ZnO nanoheterostructures for enhanced gas sensing performances, *RSC Advances* 5 (2015) 10048–10057.

[17] X. Zhou, J. Y. Liu, C. Wang, P. Sun, X. L. Hu, X. W. Li, K. Shimanoe, N. Yamazoe, C. Y. Lu, Highly sensitive acetone gas sensor based on porous $ZnFe_2O_4$ nanospheres, *Sensors and Actuators B* 206 (2015) 577–583.

[18] J. Jeong, J. H. Min, A. Y. Song, J. S. Lee, J. S. Ju, J. H. Wu, Y. K. Kim, Nonaqueous synthesis and magnetic properties of $ZnFe_2O_4$ nanocrystals with narrow size distributions, *Journal of Applied Physics* 109 (2011) 07B511.

[19] N. Pinna, M. Niederberger, Surfactant-free nonaqueous synthesis of metal oxide nanostructures, *Angewandte Chemie International Edition* 47 (2008) 5292–5304.

[20] P. H. Mutin, A. Vioux, Nonhydrolytic processing of oxide-based materials: simple routes to control homogeneity, morphology, and nanostructure, *Chemistry of Materials* 21 (2009) 582–596.

[21] N. Pinna, The "benzyl alcohol route": an elegant approach towards organic–inorganic hybrid nanomaterials, *Journal of Materials Chemistry* 17 (2007) 2769–2774.

[22] F. Rechberger, G. Ilari, M. Niederberger, Assembly of antimony doped tin oxide nanocrystals into conducting macroscopic aerogel monoliths, *Chemical Communication* 50 (2014) 13138–13141.

[23] F. J. Heiliqtaq, M. J. I. Airaghi Leccardi, D. Erdem, M. J. Süess, M. Niederberger, Anisotropically structured magnetic aerogel monoliths, *Nanoscale* 6 (2014) 13213–13221.

[24] L. Luo, D. Bozyigit, V. Wood, M. Niederberger, High-quality transparent electrodes spin-cast from preformed antimony-doped tin oxide nanocrystals for thin film optoelectronics, *Chemistry of Materials* 25 (2013) 4901–4907.

[25] G. Clavel, E. Rauwel. M. G. Willinger, N. Pinna, Non-aqueous sol–gel routes applied to atomic layer deposition of oxides, *Journal of Materials Chemistry* 19 (2009) 454–462.

[26] M. Ferrari, L. Lutterotti, Method for the simultaneous determination of anisotropic residual stresses and texture by X‐ray diffraction, *Journal of Applied Physics* 76 (1994) 7246–7255.

[27] X. H. Liu, J. Zhang, X. Z. Guo, S. H. Wu, S. R. Wang, Amino acid-assisted one-pot assembly of Au, Pt nanoparticles onto one-dimensional ZnO microrods, *Nanoscale* 2 (2010) 1178–1184.

[28] T. Yamashita, P. Hayes, Analysis of XPS spectra of Fe^{2+} and Fe^{3+} ions in oxide materials, *Applied Surfaces Science* 254 (2008) 2441–2449.

[29] Y. J. Kwon, H. G. Na, S. Y. Kang, S. W. Choi, S. S. Kim, H. W. Kim, Selective detection of low concentration toluene gas using Pt-decorated carbon nanotubes sensors, *Sensors and Actuators B* 227 (2016) 157-168.

[30] F. Li, C. Li, L. H. Zhu, W. B. Guo, L. Shen, S. P. Wen, S. P. Ruan, Enhanced toluene sensing performance of gold-functionalized $WO_3 \cdot H_2O$ nanosheets, *Sensors and Actuators B* 223 (2016) 761-767.

[31] S. Yang, Y. L. Liu, W. Chen, W. Jin, J. Zhou, H. Zhang, G. S. Zakharova, High sensitivity and good selectivity of ultralong MoO_3 nanobelts for trimethylamine gas,

Sensors and Actuators B 226 (2016) 478-485.

[32] T. Wanger, S. Haffer, C. Weinberger, D. Klaus, M. Tiemann, Mesoporous materials as gas sensors, *Chemical Society Review* 42 (2013) 4036–4053.

[33] Y. F. Sun, S. B. Liu, F. L. Meng, J. Y. Liu, Z. Jin, L. T. Kong, J. H. Liu, Metal oxide nanostructures and their gas sensing properties: a review, *Sensors* 12 (2012) 2610–2631.

Biographies

Chengjun Dong received his PhD in Materials Physics and Chemistry from Jilin University, China, in 2013. During pursuing his doctoral degree, he was a visitor in Collins research group at University of California, Irvine from 2011-2013. Since 2013, he has been working at the School of Materials Science and Engineering, Yunnan University, China. His current research activities include the synthesis of functional materials and their applications for chemical and biochemical sensors.

Xu Liu received his B.S. degree in School of Materials Science and Engineering from Yunnan University in 2015. He is currently a graduate student in Yunnan University and devotes to nanostructured metal oxides and their applications in gas sensors and supercapacitor.

Xuechun Xiao is currently a PhD student in Yunnan University and devotes to nanostructured functional materials and their applications in gas sensors and biochemical sensors.

Shangfeng Du received his BEng (1999) degree in Materials Science and Engineering from Tsinghua University and his PhD degree (2005) in Chemical Engineering from the Institute of Process Engineering, Chinese Academy of Sciences, China. He joined the Centre for Hydrogen and Fuel Cell Research (former Fuel Cells Research Group) in the School of Chemical Engineering at the University of Birmingham, as a Marie Curie Research Fellow sponsored by European Commission. His Research interests lies in the interdisciplinary area of materials science and nanotechnology, and in particular on the development of multi-functional nanostructured materials for fuel cell electrodes.

Yude Wang obtained his M.S. degree in Physics Condensed State from Yunnan University in 1997 and Ph.D. in Materials Physics and Chemistry from Tsinghua University in 2003. From 2005 to 2007, he was a guest scientist in Max-Planck-Institute of Metal and an Alexander von Humboldt fellow in Max-Planck-Institute of Colloids and Interfaces, Germany. Currently, he is a professor at the Department of Physics, Yunnan University. His work is devoted to chemical and biochemical sensors, nanostructured functional materials and their applications.

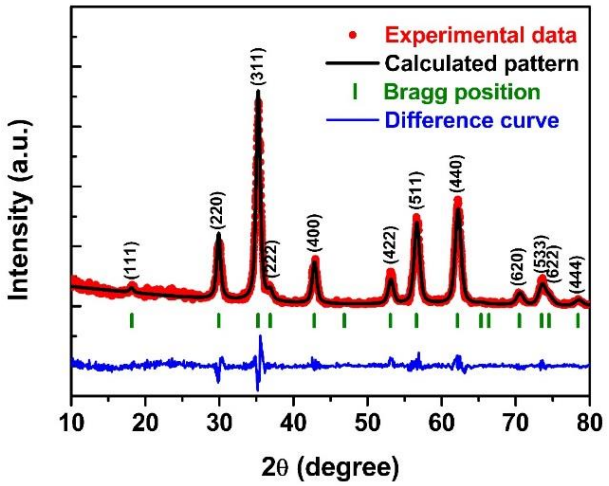

Fig. 1 XRD Rietveld refined patterns (calculated pattern (black) and difference curve (blue)) with the experimental data (Red) of $ZnFe_2O_4$ nanospheres. The olive short vertical bars stand for the positions of the Bragg reflections.

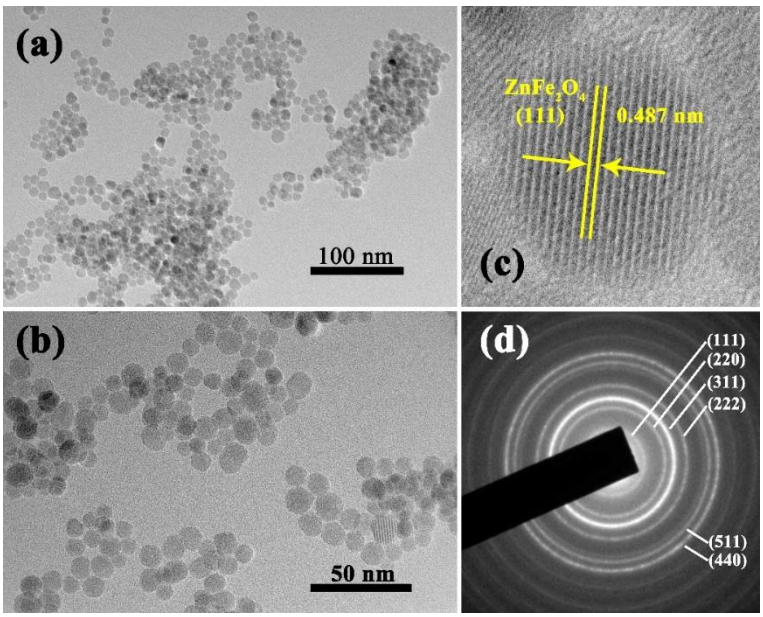

Fig. 2 Low-magnification (a) and high-magnification (b) TEM images of $ZnFe_2O_4$ nanospheres. The HRTEM image of an individual $ZnFe_2O_4$ nanosphere (c) and the corresponding SAED pattern (d).

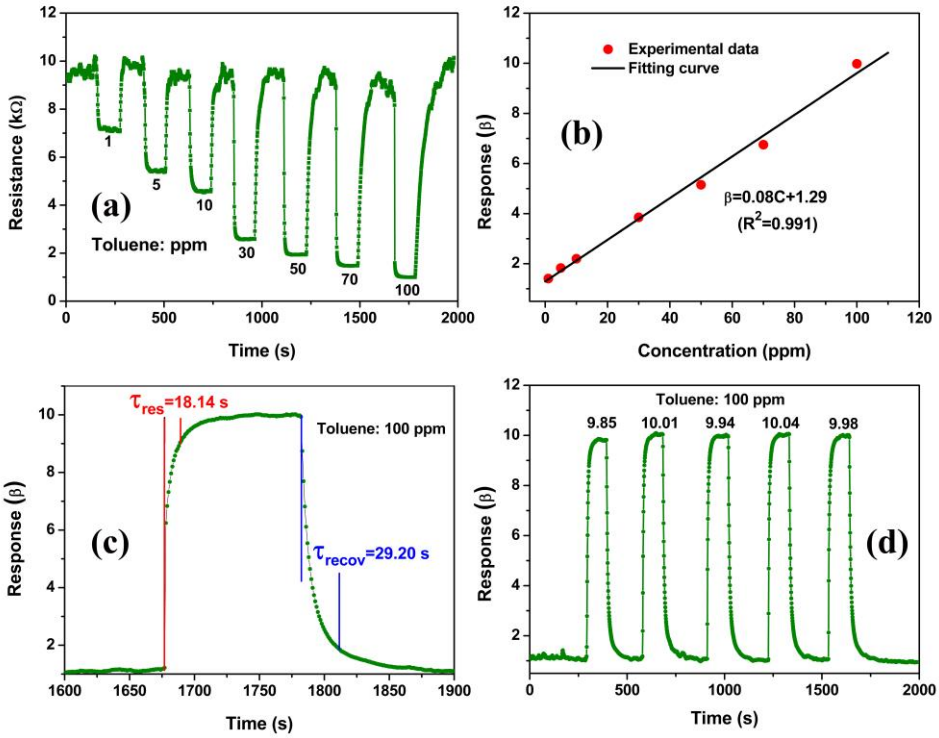

Fig. 3 (a) The dynamic resistance of $ZnFe_2O_4$ based sensor to toluene gas within the concentration range of 1-100 ppm. (b) The relationship between the gas response and toluene concentration. (c) The typical response and recovery time of $ZnFe_2O_4$ sensor to 100 ppm toluene gas. (d) Reproducibility of $ZnFe_2O_4$ sensor on successive exposure to 100 ppm toluene gas with 5 cycles. (All the tests were operated at 300 °C.)

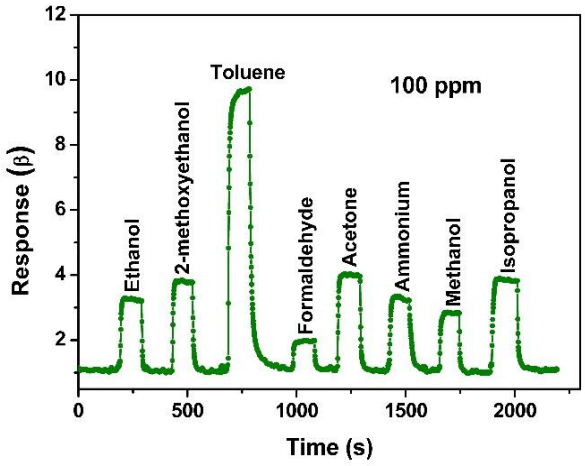

Fig. 4 Selectivity of the $ZnFe_2O_4$ based sensor to various gases with a concentration of 100 ppm at 300 ^oC.

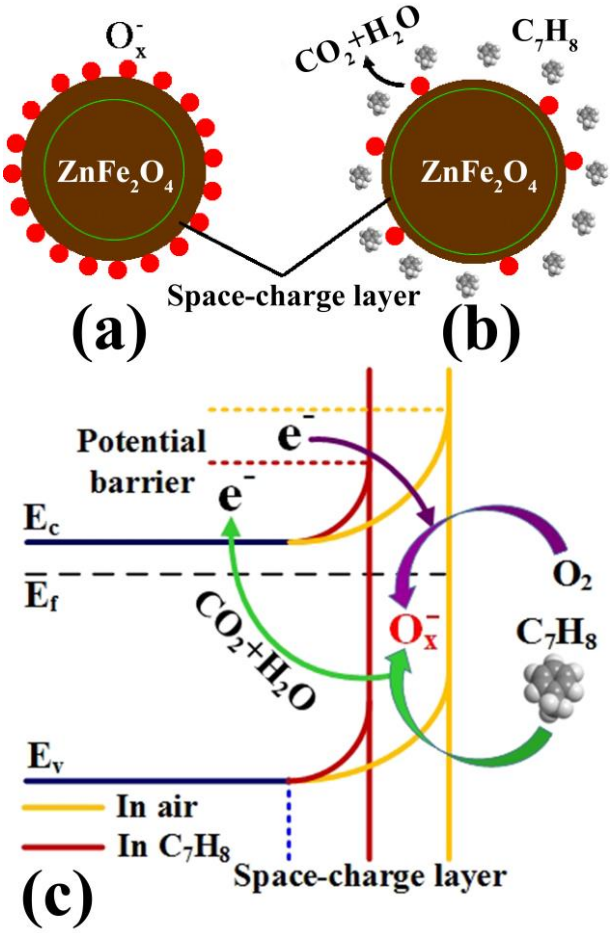

Fig. 5 Schematic diagram of the mechanism for toluene gas sensing in air (a) and toluene (b) with a contrastive change (c).